Environmental Science & Technology

Article

Cite This: Environ. Sci. Technol. 2018, 52, 12943−12951

pubs.acs.org/est

Primary Particulate Matter Emitted from Heavy Fuel and Diesel Oil Combustion in a Typical Container Ship: Characteristics and Toxicity

Di Wu,[†] Qing Li,[*,†,‡] Xiang Ding,[†] Jianfeng Sun,[†] Dan Li,[†] Hongbo Fu,[†] Monique Teich,[†] Xingnan Ye,[†] and Jianmin Chen[*,†,‡]

[†]Shanghai Key Laboratory of Atmospheric Particle Pollution and Prevention, Department of Environmental Science and Engineering, Institute of Atmospheric Sciences, Fudan University, Shanghai 200433, China

[‡]Shanghai Institute of Eco-Chongming (SIEC), No. 3663 Northern Zhongshan Road, Shanghai 200062, China

Supporting Information

ABSTRACT: Container ships have been widely recognized as an important emission source within maritime transport. Heavy fuel oil (HFO) and diesel oil (DO) are the two most commonly used fuels. This study reports the characteristics and toxicities of particulate matter (PM) emissions from HFO and DO combustion in a typical container ship. The PM number size distribution possesses a bimodal structure with peaks at ∼20 nm and ∼100 nm. The $PM_{2.5}$ emission factors (EFs) are 3.15 ± 0.39 and 0.92 ± 0.02 g/kg fuel for HFO and DO, respectively. The benzo[a]pyrene equivalent carcinogenic potency (BaP_{eq}) of 16 polycyclic aromatic hydrocarbons contained in HFO and DO $PM_{2.5}$ is approximately 0.81 ± 0.10 and 0.12 ± 0.04 mg/kg fuel, respectively. BaP_{eq} concentration shows an increasing tendency with decreased PM size. The reactive oxygen species activity and cytotoxicity of HFO $PM_{2.5}$ samples are ∼2.1 and ∼2.5 times higher than those of DO $PM_{2.5}$ samples, respectively. These health risks are both significantly attributed to the BaP_{eq} content in $PM_{2.5}$ with correlations of 0.86−0.92. Furthermore, the examined biological effects are much greater than those of atmospheric $PM_{2.5}$ collected in Shanghai. Our results imply that better fuel quality is important for improving air quality and reducing health risks.

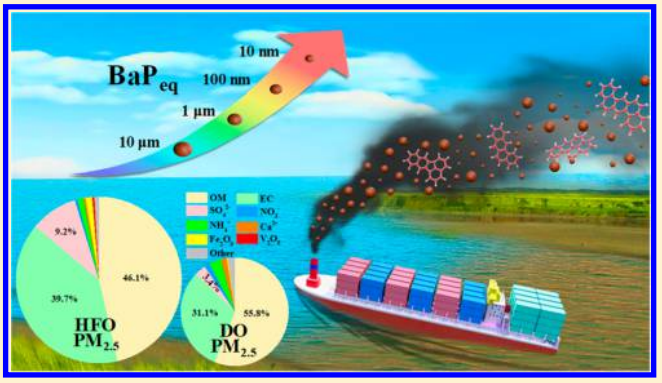

INTRODUCTION

Maritime transport plays a vital role in global trade. Pollutants emitted from ships have been widely recognized as one of the important anthropogenic emission sources.[1−4] The relative impact of ship emissions has been increasing in coastal regions.[2,5,6] Ships have the potential to contribute significantly to atmospheric particulate matter (PM) pollution in coastal regions. The contribution from shipping to atmospheric $PM_{2.5}$ (PM with an aerodynamic diameter ≤2.5 μm) levels ranges between 1 and 14% in European coastal areas.[7−9] The contribution can be higher in port cities, such as 20% in Genoa[10] and 19.5−31.7% in Cape Dorset in Canada.[11] Components of air pollution have attracted growing attention owing to many of their negative impacts, especially on human health; notably, approximately 60,000 premature deaths in 2007 accounted for $PM_{2.5}$.[12] High quality marine fuels will mitigate ship-related premature mortality by 34% and morbidity by 54%.[13]

China has more than 400 ports, 7 of which are among the world's top 10 busiest ports.[14] Several studies on ship emission inventories have recently been conducted to evaluate contributions of ship emissions to air qualities in coastal cities in China. The contributions of ship activities to $PM_{2.5}$ concentrations were estimated to be 5.3% in Shanghai,[15] 2.94% in Bohai Rim,[16] and approximately 25% in Hong Kong.[17] However, there is still a lack of ship emission factors (EFs) from Chinese harbors to be used in emission inventories. Owing to the difference of vessel types, fuel quality standards, and fuel types[18] between China and other countries, the lack of PM characteristics and EFs for Chinese ships causes a high uncertainty in estimating their impacts on local air quality.

Fuel quality plays a major role in the properties and variability of PM emissions.[19−21] Ships using residual oil have been observed to emit more PMs in the range of 0.1−0.3 μm than those using marine diesel.[22] The number size distribution of PM in ship plumes has been revealed to be dominated by the submicron size fraction.[7,17,23−26] Compared with numerous studies of size-segregated PM in the ambient atmosphere and other sources emissions, there is limited information regarding the difference in the properties of PM emissions from container ships. Therefore, both the chemical characteristics and size distribution of PM emitted from ships need to

Received: August 10, 2018
Revised: October 11, 2018
Accepted: October 12, 2018
Published: October 12, 2018

DOI: 10.1021/acs.est.8b04471
Environ. Sci. Technol. 2018, 52, 12943−12951

be studied in the field to improve the understanding of such variables.

Most maritime traffic involves the utilization of heavy fuel oil (HFO); this fuel can generate a high amount of fine and ultrafine PM, which contains organic carbon (OC), elemental carbon (EC), transition metals, and polycyclic aromatic hydrocarbons (PAHs).[27−30] There are very limited field-based studies on the effect of oil quality on PM emissions.[25,26,31] Epidemiology studies have reported that the chemical components of fine PM, including EC, OC, metals and PAHs, can induce biological effects, such as oxidative stress and cytotoxicity.[32,33] Previous studies have commonly focused on using atmospheric and health risk models to determine PM concentrations and estimate the premature mortality of regional shipping-related health impacts,[34,35] particularly in European regions or the western United States. However, no report has explained the relationship among fuel quality, chemical characteristics of PM, and toxicity effect. With the limited current knowledge, the mechanism and extent to which such exhausts affect human health have not been revealed. Hence, a detailed quantitative field study of PM emissions and their toxicity effect would be highly significant.

Aiming at identifying the influence of fuel qualities on PM emission characteristics and their toxicity effects, this study systematically investigated the chemical compositions and toxicity effects of PM emitted from a typical marine diesel engine with typical operating conditions. One type of HFO and one type of DO, as two typical marine fuels, were comparatively operated in one typical container ship. The physical characteristics (including the PM number size distribution and morphology) and chemical characteristics of size-segmented PM samples were analyzed. Toxicity effects, including oxidative stress and cytotoxicity, were further evaluated in experiments and analyzed based on their correlation with chemical composition.

MATERIALS AND METHODS

Tested Container Ship and Campaign Route. One bulk cargo ship, representative of modern container ships in China, was selected for the field study in the coastal area of Shanghai (see Figure S1). The length and width of the selected ship (a gross tonnage of ∼1925, a capacity of ∼182 TEUs) are 83.5 and 12.6 m, respectively. The main propulsion engine is a 4-stroke six-cylinder in-line medium-speed marine diesel engine ($GA6300ZC_A$, build: Ningbo Power and Machinery Group Co., Ltd.). The engine's rated power is 735 kW, and its speed is 500 rpm. During the sampling period, the engine load was stable during operation at ∼80% of maximum power, approximately 380 rpm.

The vessel carried goods along the Yangtze River channel from Daishan (30.14° N, 122.09° E) to Taicang (31.46° N, 121.13° E). The campaign route is illustrated in Figure S2. The vessel started on June 18th, 2017, in the Qugang Harbor in Daishan, crossed Hangzhou Bay, and finally arrived at Taicang, Jiangsu province, along the Yangtze River waterway. During the campaign, the same engine was tested with HFO and DO combustion in Hangzhou Bay and the Yangtze River, respectively. The fuel change took approximately 30 min when the ship entered the Yangtze River waterway. The viscosity was 19.30 mm^2/s for HFO and 2.93 mm^2/s for DO at 40 °C. The carbon residue and content of ash and vanadium(V) were lower for DO than those for HFO, as described in Table 1.

Table 1. Major Fuel Specifications

compound/property	heavy fuel oil	diesel oil
carbon (%)	85.70	80.02
hydrogen (%)	11.28	11.16
nitrogen (%)	0.17	0.08
sulfur content (%)	2.07	0.12
iron (mg/kg)	56.43	1.24
vanadium (mg/kg)	3.22	<1
chloride (mg/kg)	59	<50
water (%)	0.14	0.12
ash content (%)	0.005	0.005
flash point (°C)	66.0	74.0
viscosity @40 °C (mm^2/s)	19.30	2.93
higher heating value (J/g)	58074.2	60564.8
lower heating value (J/g)	54772.5	57366.0

Field Sampling Method. The sampling system is shown schematically in Figure S3. A flue gas analyzer (Testo 350, Germany) was employed to monitor gaseous pollutants, including CO, NO, NO_2, and SO_2. The flue gas analyzer was zeroed using standard air before sampling. The average EFs for these gaseous pollutants (i.e., CO, NO, NO_2, and SO_2) during HFO combustion were 11.90 ± 1.26, 51.59 ± 6.53, 1.93 ± 0.24, and 28.63 ± 4.23 g/kg fuel, respectively, while for DO combustion, the average EFs were 11.94 ± 1.08, 58.15 ± 2.70, 2.83 ± 0.19, and 14.19 ± 0.59 g/kg fuel, respectively. Volatile organic compounds (VOCs) were sampled via a polyvinyl fluoride film sampling bag (Tedlar, DuPont, USA) with a standard volume of 3.0 L. Samples were concentrated by a preconcentrator (Entech 7100, Entech Inc., USA), and then after examined by gas chromatography/mass spectrometry (6890GC-5973MS, Agilent, USA).

A flue gas sampler (Dekati model 4000, Finland) was employed as the online dilution system with a dilution ratio of 1:40. A scanning mobility particle sizer (SMPS, TSI 3082, USA) with a condensation particle counter (TSI 3775, USA) was employed to examine the PM size distributions in the range of 10−500 nm. SMPS were performed with consecutive runs in each operating condition more than 1 h. The total suspended PMs were sampled by a homemade particulate sampler, while the $PM_{2.5}$ samples were collected on quartz fiber filters (QFFs, Whatman 1851-865, UK) using a $PM_{2.5}$ cyclone (2000-30EH, URG Inc.). Additionally, samples on Teflon filters (Whatman 7592-104, UK) were collected for each fuel type for subsequent gravimetric, water-soluble ion and elemental analysis. Size-segregated PM samples ranging from 0.056 to 18 μm in aerodynamic diameter were collected by a micro-orifice uniform deposit impactor (MOUDI, Model 110, MSP Corp., USA) with a fixed flow rate of 30 L/min. The QFFs were preheated at 450 °C for 6 h and put in clean plastic Petri dishes before sampling, while they were reserved at −20 °C refrigerator until analysis after sampling. Three successful samples in parallel were performed for each test.

Estimation of Emission Factors. The fuel-based EFs were determined by carbon balance, using the same formula as that used in previous studies.[36] All carbon in fuels was converted to carbon-containing gaseous species (including CO_2, CO, and hydrocarbons) and carbonaceous PM during fuel combustion. CO_2 EF (EF_{CO2}, g/kg fuel) was calculated via the following equation $EF_{CO_2} = c_F \times \Delta(CO_2)/\Delta(c_{CO_2}) + \Delta(c_{CO}) + \Delta(c_{PM}) + \Delta(c_{VOCs})$, where c_F is the mass ratio of carbon in fuel (gC/kg fuel), while Δc_{CO2}, Δc_{CO}, Δc_{PM}, and

DOI: 10.1021/acs.est.8b04471
Environ. Sci. Technol. 2018, 52, 12943−12951

Δc_{VOCs} represent the concentrations of CO_2, CO, PM, and VOCs, respectively, with the background concentrations subtracted (g/m^3). Other gaseous species EFs were calculated via the equation $EF_X = EF_{CO_2} \times \Delta(X)/\Delta(CO_2)$, where EF_X is the fuel-based EF for species X, and $\Delta(X)$ represents the concentration of species X.

Transmission Electron Microscopy Analysis. Copper 230-mesh transmission electron microscopy (TEM) grids were fixed in the center of an impactor sampler to collect PMs in flue plume. The morphology of individual carbonaceous PMs was investigated by TEM. The microstructure and components of single carbonaceous PMs were analyzed by EDS and selected-area electron diffraction, as well as a field emission high-resolution TEM (FE-HRTEM, JEOL-2100F) equipped with an Oxford EDS, as detailed in a previous work.[37]

Analysis of Chemical Compositions. Each quartz filter sample was divided into quarters and analyzed for the following chemical compounds. Sixteen US EPA priority PAHs (see Table S1) were determined via using the Agilent 6890GC-5973MS. The details for extracting and analyzing the 16 PAHs were described in our previous study.[38] BaP (benzo[a]pyrene) has been regarded as one of the most carcinogenic PAH species, and the toxic equivalent factors (TEFs) for individual PAH species relative to BaP were adopted from a previous study.[39] The cancer risk of the 16 PAHs was evaluated via BaP-equivalent carcinogenic potency (BaP_{eq}) EFs. The BaP_{eq} value is possibly a little bit higher than the actual value due to some of the gas phase PAHs possibly being adsorbed in the filters during sampling.[27]

An energy-dispersive X-ray fluorescence (XRF) spectrometry (NAS100, Nayur, China) was employed to analyze a variety of selected elemental compositions in the Teflon-filter $PM_{2.5}$ samples. The elemental densities in the samples were directly analyzed after the filter was placed on the sample stage without any sample pretreatment; the details are described elsewhere.[40] A total of 7 elements, including Si, S, Cl, K, Ca, V, and Fe, were effectively examined in this study and compared with the results obtained for blank filters.

Water-soluble ions were analyzed by examining the Teflon-filter samples via an ion chromatograph (940 Professional IC, Metrohm, Switzerland) equipped with a Metrosep A supp 16-250 separation column and a Metrosep C6 analytical column. The corresponding detection limits for major inorganic ions were within 0.47−3.33 ng/mL. Br^-, PO_4^{3-}, Li^+, and K^+ were below the detection limits. Blank levels are below MDL.

OC and EC fractions of PMs were analyzed by a thermal/optical carbon analyzer (Model 2015, Atmoslytic Inc., CA) according to the IMPROVE protocol. Four OC fractions and three EC fractions (EC1, EC2, and EC3 evolved at 580, 740, and 840 °C in a 98% He/2% O_2 atmosphere, respectively) were produced. The MDL for OC determined by using the thermal/optical carbon analyzer was 0.18 ± 0.06 μg/cm^2, while it was 0.04 ± 0.01 μg/cm^2 for EC. Blank levels are below MDL.

Evaluation of Toxicity. The cell line of an adenocarcinoma human alveolar basal epithelial (A549) was employed to measure the toxic effects of the PM samples, as described previously in detail.[41] Here we briefly outlined the analysis procedures of cell viability and oxidative stress. The PMs were extraced by methanol, and the solvent was then removed by nitrogen. The cells were exposed to PM extracts at different concentrations. After incubation for 24 h, cell viability was analyzed via using 3-(4,5-dimethylthiazol-2-yl)-2,5-diphenyltetrazolium bromide assay. The optical emission intensity of 570 nm wavelength was detected via a microplate reader (H1Multi-Mode, BioTek, Winooski, VT). The intracellular reactive oxygen species (ROS) generation was detected by dichlorofluorescein staining. The fluorescence intensity (488 and 525 nm) of the dichlorofluorescein was determined using the microplate reader. A more detailed description can be found in previous studies.[42−44] The end point of cell viability was calculated by the IC_{50} value (the concentration causing 50% inhibition of cell viability).[45] The results of oxidative stress were shown via the $EC_{1.5}$ value (1.5-fold increase in ROS generation relative to control).[46] Three successful analyses in parallel were performed for each test.

RESULTS AND DISCUSSION

Bimodal Distribution of Submicron PMs. Ship-exhaust PM number and size distributions of HFO and DO combustion in the size range 10−500 nm are characterized in Figure 1. Surface and volume distribution of PM from ship exhaust resulting from HFO and DO combustion is shown in Figure S4. Size distributions of EC+OC measured by the MOUDI were consistent with the volume distribution measured by the SMPS. The PM number size distributions for both fuels present a bimodal distribution with two distinct peaks at approximately 23 and 100 nm, respectively. These results show a similar tendency with a previous study conducted in Sweden.[47] The number distribution of DO PM is dominated by the ultrafine mode. Compared with DO PM, HFO emission has a high proportion of fine mode PM; this is possibly attributed to the incomplete combustion of HFO, which caused a large amount of oil droplets to undergo incomplete combustion and form relatively large carbonaceous particles. The mean particle diameter is smaller than that from on-road vehicle engines.[48]

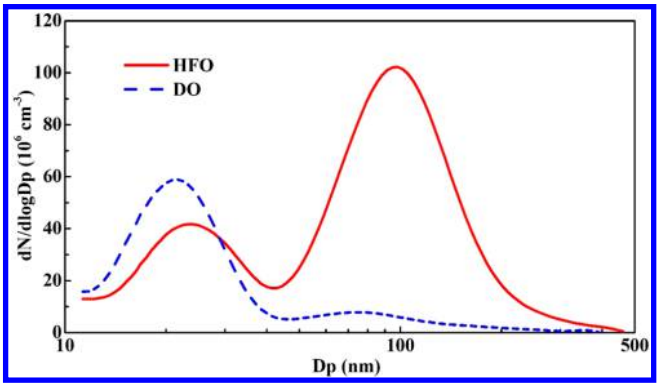

Figure 1. Number size distribution of PMs emitted from ship exhaust resulting from HFO and DO combustion.

Particle Emissions and Chemical Composition. The EFs of total suspended primary PM were 5.93 ± 1.45 g/kg and 2.02 ± 0.65 g/kg fuel for HFO and DO combustion, respectively. The EFs of total primary $PM_{2.5}$ were 3.15 ± 0.39 g/kg fuel for HFO, whereas they were 0.92 ± 0.02 g/kg fuel for DO. The EFs of primary PMs obtained in this study are in agreement with that in the literature.[49] EFs for total suspended PM and $PM_{2.5}$ showed higher values for HFO. The average EFs for *n*-alkanes resulting from HFO and DO combustion were 0.48 ± 0.08 and 0.16 ± 0.01 g/kg fuel,

DOI: 10.1021/acs.est.8b04471
Environ. Sci. Technol. 2018, 52, 12943−12951

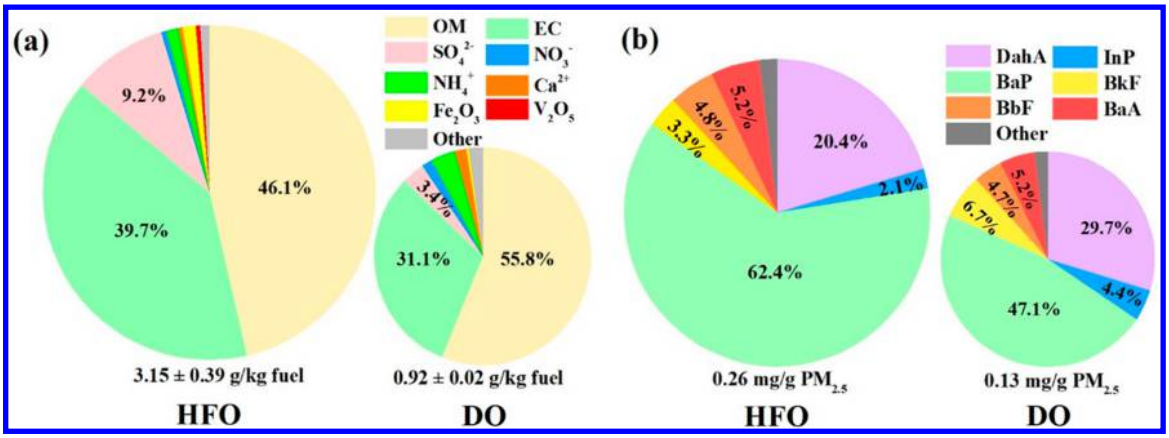

Figure 2. (a) Chemical compositions of $PM_{2.5}$ samples from HFO and DO combustion in the same ship. "Other" consists of SiO_2, F^-, Cl^-, Na^+, Mg^{2+}, and other ignorable mass fraction species. (b) Fraction of total-BaP_{eq} (benzo[a]pyrene equivalent carcinogenic potency) in HFO and DO $PM_{2.5}$ samples and individual contributions of PAHs (16 polycyclic aromatic hydrocarbons). "Other" consists of Nap, Acy, Flo, Phe, Ant, Flu, Pyr, Chry, and BghiP (with toxic equivalence factors <0.1).

respectively. The incomplete combustion process of fossil fuels can generate *n*-alkanes and release smaller than C_{26} homologues.[50] EFs for *n*-alkanes of HFO were 3-fold higher than that of DO, which indicated a large amount of incomplete combustion fuel might be emitted along with the exhaust during operation with the HFO. The noncarbonaceous components of $PM_{2.5}$ samples were mainly contributed to SO_4^{2-}, followed by NH_4^+, NO_3^-, Ca^{2+}, Fe, and V; the remaining fraction, including F^-, Cl^-, Na^+, Mg^{2+}, and SiO_2, was less than 3%. HFO $PM_{2.5}$ contained 9.2 ± 0.8% of sulfate, whereas DO $PM_{2.5}$ contained 3.4 ± 0.5%. The NH_4^+ fraction for HFO $PM_{2.5}$ was 1.2 ± 0.6%, while for DO $PM_{2.5}$ was 3.6 ± 1.3%. NH_4^+ is generated when ammonia (NH_3) reacts with proton donors, it can be inferred where NH_3 was present in the exhaust gas of ship emission. Since NH_3 has a significant impact on air quality, it is necessary to detect it in future work. The concentrations of V and Fe in HFO $PM_{2.5}$ are much higher than those for DO $PM_{2.5}$; this possibly is due to element vibrations in two types of fuels, as shown in Table 1. In mass balance calculations, metals commonly found in crustal material are assumed to present as oxides; these oxides are Fe_2O_3 and V_2O_5.

The majority of the $PM_{2.5}$ mass in HFO or DO was carbonaceous, as shown in Figure 2a. Organic matter (OM) was the major component of $PM_{2.5}$ in HFO and DO samples. OM values for HFO and DO were calculated from OC via the relationships OM = 1.26 × OC and OM = 1.50 × OC, respectively, where the coefficients used for the relationship between OM and OC were determined by full component analysis of $PM_{2.5}$, including carbonaceous and noncarbonaceous species analysis. The coefficients of OM/OC determined in the study are consistent with the frequently used values in the literature, which ranged from 1.2−1.8.[51−53] The carbonaceous mass fractions (OM+EC) for HFO were approximately 85.8%, while for DO they were 86.9%. The ratio of OC/EC in this work was 0.93 and 1.19 for HFO and DO, respectively. The lower ratio also suggests lower combustion efficiency for HFO when compared to DO. EC originates from the pyrolysis of fuel droplets. It can be easily formed at a low air-fuel ratio and high combustion temperature condition.[54] EC can be classified into char-EC and soot-EC. Char-EC is formed at a relatively low combustion temperature via the fuel pyrolysis, while soot-EC is formed at a high combustion temperature via a gas-to-particle conversion.[55] Char-EC accounted for approximately 46% of EC mass for HFO, whereas it accounted for 33% for DO.

Figure S5 and Figure S6 show the morphology and speciation of HFO and DO PM samples characterized by STEM-EDS analysis. Soot was the predominant type of EC. The HRTEM images of these particles exhibited the disordered graphitic layers with a graphic microstructure. Soot spheres showed onion-like structures. EDS results of soot PMs showed that the particles predominantly contained carbon. Nanometer-sized particles rich in S were observed at the surface of PMs or within PM agglomerates (Figures S5b and S6b). Figure S5c and Figure S 5d show high content of Fe and V in HFO PM samples, respectively. The V element can be used as a tracer of HFO combustion and was not present in the DO exhaust. Ca is the main component of the mineral PMs (Figure S6d). The difference in morphology is attributed to their different formation mechanisms.

BaP_{eq} Fraction in $PM_{2.5}$ and Size Segregated PM. Figure S7 shows the characteristics of 16 PAHs in the $PM_{2.5}$ samples. The PAH emission characteristics and EFs showed high differences during HFO and DO combustion. PAH EFs of HFO were 4.6-fold higher than that of DO (Figure S8). This result is consistent with a previous study, in which HFO contains a large fraction of aromatic compounds, typically polycyclic aromatics, while DO generally contains higher proportions of aliphatic compounds.[56] Chry dominated the PAH pattern, followed by Pyr and BaP in HFO $PM_{2.5}$; while for DO $PM_{2.5}$, Pyr dominated the PAH pattern, followed by Chry and BkF. HFO samples contained higher ring PAHs than DO samples, such as InP, DahA, and BghiP.

Figure 2b shows the Total-BaP_{eq} values of the 16 PAHs in HFO and DO $PM_{2.5}$ samples. The sum of the BaP_{eq} values for DahA, InP, BaP, BkF, BbF, and BaA (with TEF more than or equal to 0.1) contributes to ∼95% of the BaP_{eq} for a total 16 PAH species. The total-BaP_{eq} values in HFO and DO $PM_{2.5}$ samples per kg fuel mass are shown in Figure S9. The reduction in the BaP_{eq} of the DO $PM_{2.5}$ sample was 85% compared with the BaP_{eq} value of the HFO $PM_{2.5}$ sample.

Comparison of BaP_{eq} in PM exhausted from various anthropogenic emission sources is shown in Table S2. In order to give the effective comparison to BaP_{eq} from different sources, all the values were unified into mg/g PM in the study.

DOI: 10.1021/acs.est.8b04471
Environ. Sci. Technol. 2018, 52, 12943−12951

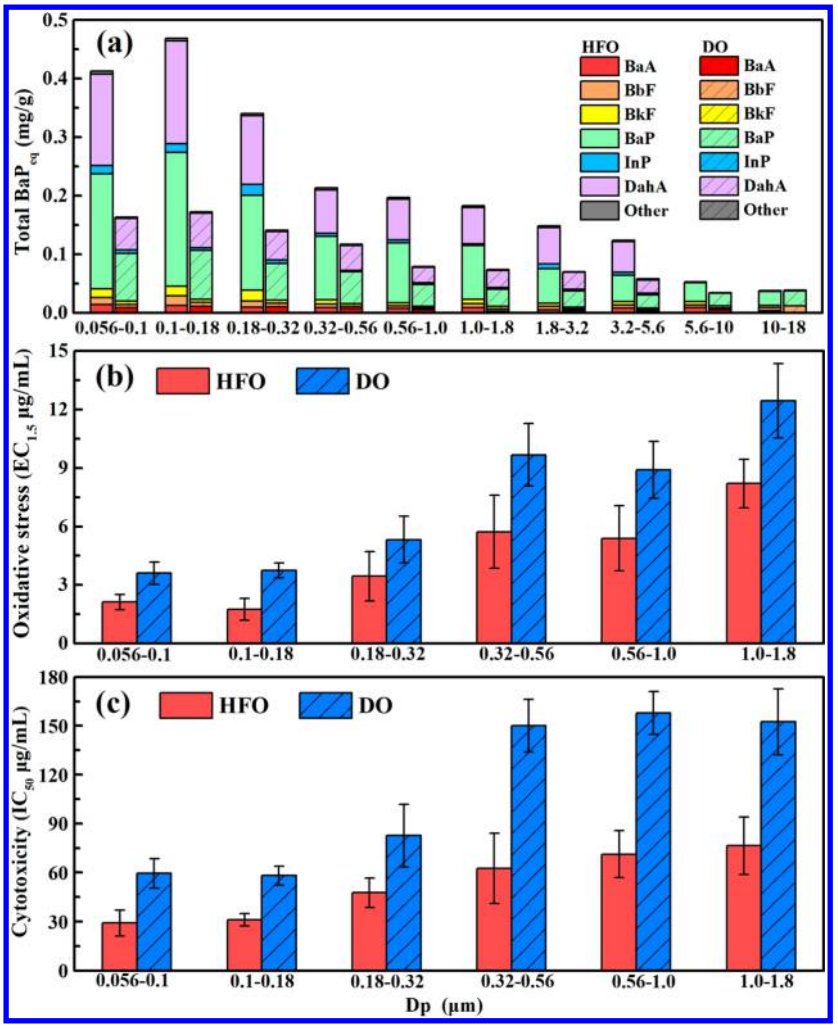

Figure 3. (a) Fraction of BaP_{eq} (benzo[a]pyrene equivalent carcinogenic potency) in HFO and DO size-segregated PM samples and individual contributions of 16 PAHs. "Other" consists of Nap, Acy, Flo, Phe, Ant, Flu, Pyr, Chry, and BghiP (with toxic equivalence factors <0.1). Exhaust PM samples were diluted to specified concentrations and then added to the cells. (b) $EC_{1.5}$ (1.5-fold increase in intracellular ROS generation relative to that in the control) and (c) IC_{50} (the concentration causing 50% inhibition of cell viability) of HFO and DO size-segregated PM samples. Smaller values are more toxic.

The results showed that the values from residential coal combustion[57] were in a much higher level than those of HFO and DO in this study. BaP_{eq} from household fuel combustion[40] varied largely with different solid fuels, which might be caused by the different fuel composition. BaP_{eq} from a container ship was slightly lower than that reported in a previous study;[58] this may be due to operating with different fuel types and marine engines. BaP_{eq} in HFO PM emitted from a container ship was much greater than those from on-road vehicle emissions, including gasoline[59] and diesel vehicles,[60,61] while the value in DO PM was higher than diesel vehicles but at the same level with gasoline vehicles. However, motorcycles showed extremely higher BaP_{eq} values than ships and other vehicles;[62] this may be due to their small combustor chamber which limits the combustion efficiency of fuels.[63] Besides, the BaP_{eq} values in the lab test were lower than those in the field test, which could underestimate the carcinogenic risk from the real-world emission. Hence, more systematic real-world measurements are urgently needed to improve the circumstances. Since BaP_{eq} from a container ship were higher than many mobile sources, the health effect caused by ships cannot be neglected especially in coastal areas.[64] Furthermore, a large amount of toxic heavy metals is also emitted from ship exhausts, which could aggravate the negative healthy impacts.[65]

The total-BaP_{eq} in HFO and DO size-segregated PM is presented in Figure 3a, where all the values were unified into mg/g PM. The total-BaP_{eq} in both HFO and DO size-segregated PM samples possesses peaks at particle aerodynamic diameters of 0.1−0.18 μm. The total-BaP_{eq} was reduced in almost all size ranges except in PM_{10-18} when operated with DO, and the three highest reductions in emissions were in $PM_{0.056-0.1}$, $PM_{0.1-0.18}$, and $PM_{0.18-0.32}$, which showed percentage reductions of 60.6%, 63.4%, and 62.1%, respectively. It has been shown that the more carcinogenic particulate PAHs are found in smaller PM from HFO and DO, indicating that at a similarly increased concentration of finer PM, the resulting particulate PAHs would have much higher carcinogenicity. This may be resulting from the larger surface area of smaller PM, which creates a higher capacity to absorb and deliver toxic chemicals. Hence, in addition to $PM_{2.5}$ emitted from ships when using HFO or DO, special attention should be paid to ultrafine PM as well. The total-BaP_{eq} values in HFO and DO PM samples per kg fuel mass are shown in Figure S10.

DOI: 10.1021/acs.est.8b04471
Environ. Sci. Technol. 2018, 52, 12943−12951

Toxicity of Primary PM. The biological effects of HFO size-segregated PMs were significantly greater than those of DO PMs. This may be due to varying chemical speciation in relation to different fuel types. Particle constituents, notably PAHs, may elicit distinct biological responses. Oxidative stress exhibited significant differences across size fractions (Figure 3b). The ROS-generating capacity in HFO and DO size-segregated PM samples possesses peaks at 0.1−0.18 μm and 0.056−0.1 μm, respectively, which is consistent with the number and size distribution of HFO and DO PM (Figure 1). The result suggests that, in addition to chemical composition, the particle number and size distribution affect redox activity. The cell viability exhibited a unique pattern of response (Figure 3c). Statistical analysis reveals that the investigation of the ultrafine fraction, whose oxidative-stress and cytotoxic effects are more evident, is highly significant. The biotoxicity of ultrafine PM was higher than that of large-sized PM, which was consistent with a previous report.[66] This may be attributed to the higher ratio of toxic chemical components, as well as the greater surface area of ultrafine particles at the same weight.[43]

Dose-dependent effects of HFO and DO $PM_{2.5}$ samples were observed in the values of $EC_{1.5}$ and IC_{50}. The $EC_{1.5}$ values for HFO $PM_{2.5}$ and DO $PM_{2.5}$ were 3.06 ± 1.28 and 6.35 ± 2.34 μg/mL, respectively, whereas the IC_{50} values were 39.6 ± 18.3 and 97.9 ± 27.8 μg/mL, respectively. It suggests that the HFO $PM_{2.5}$ would have higher negative biological effects than DO $PM_{2.5}$. PM exhausted from marine diesel engines when operated with HFO or DO induced greater toxic effects than on-road vehicle emissions, whose $EC_{1.5}$ values for diesel and petrol emitted PMs were reported to be 25 μg/mL[67] and 35 μg/mL,[68] respectively; while the IC_{50} values for petrol exhaust particles and residential solid fuel burning were 250 μg/mL[67] and 100 μg/mL,[44] respectively. The results indicate that it is of great importance to make relative regulations to avoid negative toxic effects caused by ship emissions. The toxicity and health effects might be more negative when changing to lower loads due to higher EFs of pollutants.[69] How these differences influence the toxicity and health effects need to be investigated in the future.

Correlation between BaP_{eq} and Biological Effects. Figure 4 shows the linear regression analysis of the biological effects and BaP_{eq} content in HFO and DO PM samples. The biological effects of both HFO and DO PM samples were significantly correlated (p-value <0.01) with the BaP_{eq} values, with correlation coefficients (r) of 86%, 90%, 89%, and 92% for HFO oxidative stress, DO oxidative stress, HFO cytotoxicity, and DO cytotoxicity, respectively. Furthermore, the correlations are more significant in DO samples than those in HFO samples. This is possibly owing to the higher content of other hazardous compounds in HFO PM, such as transition metals (Fe, V), which have been identified to possess significant negative potential impacts on biological effects.[65]

Environmental Implication. $PM_{2.5}$ emitted from lower-quality oil (HFO) has greater biological effects than that emitted from higher-quality oil (DO). Furthermore, both of these sources have greater negative health impacts than atmospheric $PM_{2.5}$ samples collected in January 2016 in the city of Shanghai, as shown in Figure 5. The sampling process is detailed in the SI. $EC_{1.5}$ values for the atmospheric $PM_{2.5}$ on heavy- and light-pollution days were 7.60 ± 1.51 and 16.30 ± 2.90 μg/mL, respectively, and IC_{50} values were 105 ± 20 and 319 ± 45 μg/mL, respectively. The values of HFO $PM_{2.5}$ were 2.9- and 2.5-fold higher than those of atmospheric $PM_{2.5}$ on heavily polluted days but 8.7- and 5.3-fold higher than those on lightly polluted days. It has been implied that differences in the

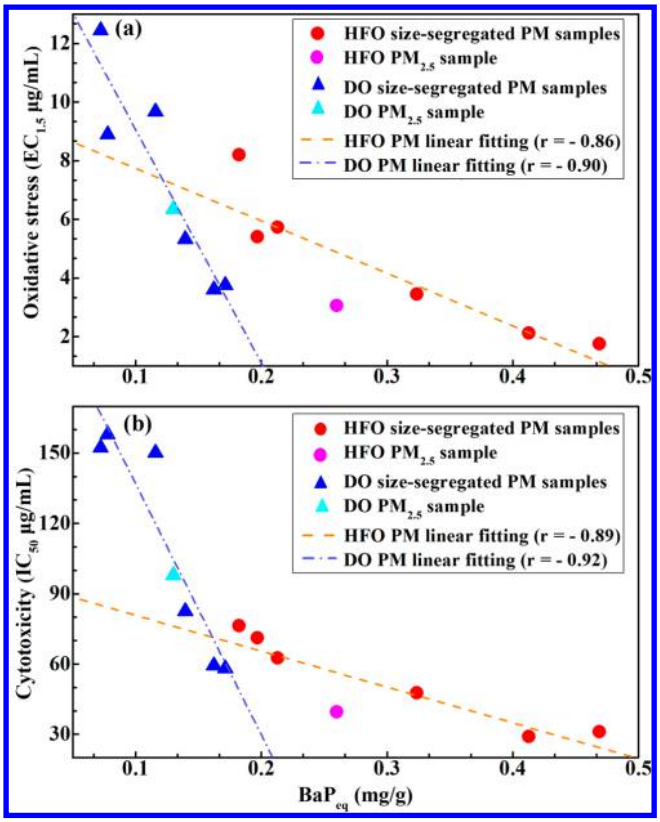

Figure 4. Linear regression analysis for the correlation between biological effects and BaP_{eq}: (a) oxidative stress and (b) cytotoxicity. The linear fit of oxidative stress has a correlation of $EC_{1.5}$ = −17.9 BaP_{eq} + 9.5 for HFO and $EC_{1.5}$ = −79.6 BaP_{eq} + 17.0 for DO, while that of cytotoxicity has a relationship of IC_{50} = −153.2 BaP_{eq} + 96.2 for HFO and IC_{50} = −1085.6 BaP_{eq} + 243.1 for DO. The correlation coefficients (r) for the four correlations are −0.86, −0.90, −0.89, and −0.92, respectively, while the p-values are 0.009, 0.006, 0.008, and 0.003, respectively.

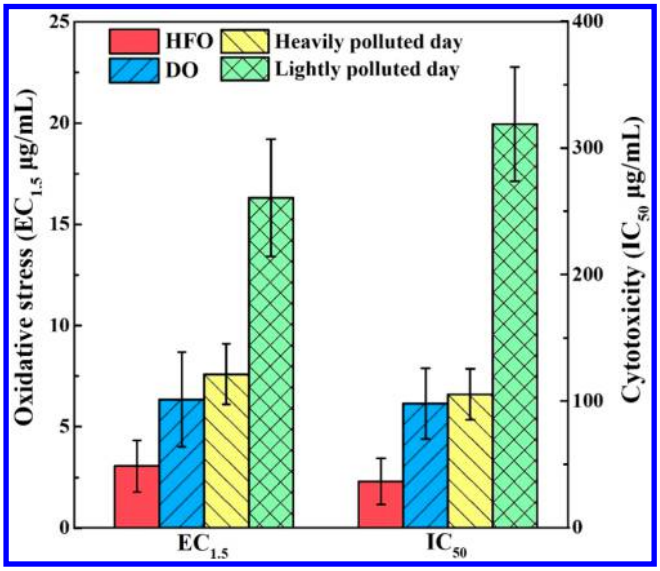

Figure 5. Comparison of oxidative stress and cytotoxicity for $PM_{2.5}$ samples from ship emissions and atmospheric air in December 2016, Shanghai. Smaller values are more toxic.

DOI: 10.1021/acs.est.8b04471
Environ. Sci. Technol. 2018, 52, 12943−12951

amounts of specific substances associated with particles emitted from container ships could lead to greater oxidative stress and cytotoxicity.

The implications drawn from this field study are that the negative impacts from HFO-operated container ships need to be mitigated and that HFO should be replaced by high-quality refined fuels (high heating value and lower sulfur content fuel) to reduce negative environmental impacts and low effect of public health, particularly in coastal areas and harbor cities. A reduction in the PAH emissions could lead to a reduction of ~85% in BaP_{eq}, which would alleviate potential biological effects. Hence, further regulation of fuel quality (sulfur, aromatic hydrocarbons) is implied to be an effective approach to achieve air quality and health targets by jointly reducing PM and health impacts from shipping emissions. Although DO is a low-sulfur fuel and is widely consumed in sulfur-emission control areas, PM emitted from ships when using DO should not be neglected due to its greater toxic effect relative to atmospheric PM. Futhermore, it is necessary to consider standards based on particle number owing to the differing toxicity of ultrafine PM.

■ ASSOCIATED CONTENT

Supporting Information

The Supporting Information is available free of charge on the ACS Publications website at DOI: 10.1021/acs.est.8b04471.

Ten figures, two tables, and description of atmospheric $PM_{2.5}$ samples collected in Shanghai in 2016 (PDF)

■ AUTHOR INFORMATION

Corresponding Authors

*E-mail: qli@fudan.edu.cn (Q.L.).
*E-mail: jmchen@fudan.edu.cn (J.C.).

ORCID

Qing Li: 0000-0003-0587-1748
Dan Li: 0000-0001-6765-6627

Notes

The authors declare no competing financial interest.

■ ACKNOWLEDGMENTS

This work was supported by the Ministry of Science and Technology of China (2016YFC0202700 and 2018YFC0213800), the National Natural Science Foundation of China (91743202 and 21527814), and the Natural Science Foundation of Shanghai (18ZR1403000).

■ REFERENCES

(1) Yau, P. S.; Lee, S. C.; Corbett, J. J.; Wang, C.; Cheng, Y.; Ho, K. F. Estimation of Exhaust Emission from Ocean-Going Vessels in Hong Kong. *Sci. Total Environ.* **2012**, *431* (5), 299−306.

(2) Eyring, V.; Isaksen, I. S. A.; Berntsen, T.; Collins, W. J.; Corbett, J. J.; Endresen, O.; Grainger, R. G.; Moldanova, J.; Schlager, H.; Stevenson, D. S. Transport Impacts on Atmosphere and Climate: Shipping. *Atmos. Environ.* **2010**, *44* (37), 4735−4771.

(3) Endresen, Ø. Emission from International Sea Transportation and Environmental Impact. *J. Geophys. Res.* **2003**, *108* (D17), 4560.

(4) Liu, H.; Fu, M.; Jin, X.; Shang, Y.; Shindell, D.; Faluvegi, G.; Shindell, C.; He, K. Health and Climate Impacts of Ocean-Going Vessels in East Asia. *Nat. Clim. Change* **2016**, *6* (11), 1037−1041.

(5) Lu, G.; Brook, J. R.; Rami Alfarra, M.; Anlauf, K.; Richard Leaitch, W.; Sharma, S.; Wang, D.; Worsnop, D. R.; Phinney, L. Identification and Characterization of Inland Ship Plumes over Vancouver, Bc. *Atmos. Environ.* **2006**, *40* (15), 2767−2782.

(6) Becagli, S.; Sferlazzo, D. M.; Pace, G.; di Sarra, A.; Bommarito, C.; Calzolai, G.; Ghedini, C.; Lucarelli, F.; Meloni, D.; Monteleone, F.; Severi, M.; Traversi, R.; Udisti, R. Evidence for Heavy Fuel Oil Combustion Aerosols from Chemical Analyses at the Island of Lampedusa: A Possible Large Role of Ships Emissions in the Mediterranean. *Atmos. Chem. Phys.* **2012**, *12* (7), 3479−3492.

(7) Donateo, A.; Gregoris, E.; Gambaro, A.; Merico, E.; Giua, R.; Nocioni, A.; Contini, D. Contribution of Harbour Activities and Ship Traffic to Pm2.5, Particle Number Concentrations and Pahs in a Port City of the Mediterranean Sea (Italy). *Environ. Sci. Pollut. Res.* **2014**, *21* (15), 9415−29.

(8) Viana, M.; Hammingh, P.; Colette, A.; Querol, X.; Degraeuwe, B.; Vlieger, I. d.; van Aardenne, J. Impact of Maritime Transport Emissions on Coastal Air Quality in Europe. *Atmos. Environ.* **2014**, *90*, 96−105.

(9) Viana, M.; Fulvio, A.; Andres, A.; Xavier, Q.; Teresa, M. Chemical Tracers of Particulate Emissions from Commercial Shipping. *Environ. Sci. Technol.* **2009**, *43*, 7472−7477.

(10) Mazzei, F.; D'Alessandro, A.; Lucarelli, F.; Nava, S.; Prati, P.; Valli, G.; Vecchi, R. Characterization of Particulate Matter Sources in an Urban Environment. *Sci. Total Environ.* **2008**, *401* (1), 81−89.

(11) Aliabadi, A. A.; Staebler, R. M.; Sharma, S. Air Quality Monitoring in Communities of the Canadian Arctic During the High Shipping Season with a Focus on Local and Marine Pollution. *Atmos. Chem. Phys.* **2015**, *15* (5), 2651−2673.

(12) Corbett, J. J.; Winebrake, J. J.; Green, E. H.; Kasibhatla, P.; Eyring, V.; Lauer, A. Mortality from Ship Emissions: A Global Assessment. *Environ. Sci. Technol.* **2007**, *41* (24), 8512.

(13) Sofiev, M.; Winebrake, J. J.; Johansson, L.; Carr, E. W.; Prank, M.; Soares, J.; Vira, J.; Kouznetsov, R.; Jalkanen, J. P.; Corbett, J. J. Cleaner Fuels for Ships Provide Public Health Benefits with Climate Tradeoffs. *Nat. Commun.* **2018**, *9* (1), 406.

(14) Zhang, Y.; Yang, X.; Brown, R.; Yang, L.; Morawska, L.; Ristovski, Z.; Fu, Q.; Huang, C. Shipping Emissions and Their Impacts on Air Quality in China. *Sci. Total Environ.* **2017**, *581*−*582*, 186−198.

(15) Fu, M.; Ding, Y.; Ge, Y.; Yu, L.; Yin, H.; Ye, W.; Liang, B. Real-World Emissions of Inland Ships on the Grand Canal, China. *Atmos. Environ.* **2013**, *81* (4), 222−229.

(16) Zhang, F.; Chen, Y.; Tian, C.; Wang, X.; Huang, G.; Fang, Y.; Zong, Z. Identification and Quantification of Shipping Emissions in Bohai Rim, China. *Sci. Total Environ.* **2014**, *497*−*498* (Supplement C), 570−577.

(17) Yau, P. S.; Lee, S. C.; Cheng, Y.; Huang, Y.; Lai, S. C.; Xu, X. H. Contribution of Ship Emissions to the Fine Particulate in the Community near an International Port in Hong Kong. *Atmos. Res.* **2013**, *124* (2), 61−72.

(18) Zhang, F.; Chen, Y.; Tian, C.; Lou, D.; Li, J.; Zhang, G.; Matthias, V. Emission Factors for Gaseous and Particulate Pollutants from Offshore Diesel Engine Vessels in China. *Atmos. Chem. Phys.* **2016**, *16* (10), 6319−6334.

(19) Alander, T. J.; Leskinen, A. P.; Raunemaa, T. M.; Rantanen, L. Characterization of Diesel Particles: Effects of Fuel Reformulation, Exhaust Aftertreatment, and Engine Operation on Particle Carbon Composition and Volatility. *Environ. Sci. Technol.* **2004**, *38* (9), 2707−2714.

(20) Ntziachristos, L.; Saukko, E.; Lehtoranta, K.; Rönkkö, T.; Timonen, H.; Simonen, P.; Karjalainen, P.; Keskinen, J. Particle Emissions Characterization from a Medium-Speed Marine Diesel Engine with Two Fuels at Different Sampling Conditions. *Fuel* **2016**, *186*, 456−465.

(21) Lack, D. A.; Cappa, C. D.; Langridge, J.; Bahreini, R.; Buffaloe, G.; Brock, C.; Cerully, K.; Coffman, D.; Hayden, K.; Holloway, J.; Lerner, B.; Massoli, P.; Li, S. M.; McLaren, R.; Middlebrook, A. M.; Moore, R.; Nenes, A.; Nuaaman, I.; Onasch, T. B.; Peischl, J.; Perring, A.; Quinn, P. K.; Ryerson, T.; Schwartz, J. P.; Spackman, R.; Wofsy, S. C.; Worsnop, D.; Xiang, B.; Williams, E. Impact of Fuel Quality Regulation and Speed Reductions on Shipping Emissions: Implica-

DOI: 10.1021/acs.est.8b04471
Environ. Sci. Technol. 2018, 52, 12943−12951

tions for Climate and Air Quality. *Environ. Sci. Technol.* **2011**, *45* (20), 9052−9060.
(22) Sinha, P.; Hobbs, P. V.; Yokelson, R. J.; Christian, T. J.; Kirchstetter, T. W.; Bruintjes, R. Emissions of Trace Gases and Particles from Two Ships in the Southern Atlantic Ocean. *Atmos. Environ.* **2003**, *37* (15), 2139−2148.
(23) Petzold, A.; Hasselbach, J.; Lauer, P.; Baumann, R.; Franke, K.; Gurk, C.; Schlager, H.; Weingartner, E. Experimental Studies on Particle Emissions from Cruising Ship Their Characteristic Properties Transformation and Atmospheric Lifetime in the Marine Boundary Layer. *Atmos. Chem. Phys.* **2008**, *8*, 2387−2403.
(24) Chen, D.; Wang, X.; Nelson, P.; Li, Y.; Zhao, N.; Zhao, Y.; Lang, J.; Zhou, Y.; Guo, X. Ship Emission Inventory and Its Impact on the Pm 2.5 Air Pollution in Qingdao Port, North China. *Atmos. Environ.* **2017**, *166*, 351−361.
(25) Moldanová, J.; Fridell, E.; Winnes, H.; Holminfridell, S. Physical and Chemical Characterisation of Pm Emissions from Two Ships Operating in European Emission Control Areas. *Atmos. Meas. Tech.* **2013**, *6* (12), 3577−3596.
(26) Winnes, H.; Fridell, E. Particle Emissions from Ships: Dependence on Fuel Type. *J. Air Waste Manage. Assoc.* **2009**, *59* (12), 1391−1398.
(27) Murphy, S. M.; Agrawal, H.; Sorooshian, A.; Padró, L. T.; Gates, H.; Hersey, S.; Welch, W. A.; Jung, H.; Miller, J. W.; Iii, D. R. C. Comprehensive Simultaneous Shipboard and Airborne Characterization of Exhaust from a Modern Container Ship at Sea. *Environ. Sci. Technol.* **2009**, *43* (13), 4626−4640.
(28) Moldanová, J.; Fridell, E.; Popovicheva, O.; Demirdjian, B.; Tishkova, V.; Faccinetto, A.; Focsa, C. Characterisation of Particulate Matter and Gaseous Emissions from a Large Ship Diesel Engine. *Atmos. Environ.* **2009**, *43* (16), 2632−2641.
(29) Agrawal, H.; Welch, W. A.; Miller, J. W.; Cocker, D. R. Emission Measurements from a Crude Oil Tanker at Sea. *Environ. Sci. Technol.* **2008**, *42* (19), 7098−7103.
(30) Agrawal, H.; Malloy, Q. G. J.; Welch, W. A.; Wayne Miller, J.; Cocker, D. R. In-Use Gaseous and Particulate Matter Emissions from a Modern Ocean Going Container Vessel. *Atmos. Environ.* **2008**, *42* (21), 5504−5510.
(31) Lack, D. A.; Corbett, J. J. Black Carbon from Ships: A Review of the Effects of Ship Speed, Fuel Quality and Exhaust Gas Scrubbing. *Atmos. Chem. Phys.* **2012**, *12* (9), 3985−4000.
(32) Son, J. Y.; Lee, J. T.; Kim, K. H.; Jung, K.; Bell, M. L. Characterization of Fine Particulate Matter and Associations between Particulate Chemical Constituents and Mortality in Seoul, Korea. *Environ. Health Perspect.* **2012**, *120* (6), 872−878.
(33) Tian, L.; Ho, K.-f.; Louie, P. K. K.; Qiu, H.; Pun, V. C.; Kan, H.; Yu, I. T. S.; Wong, T. W. Shipping Emissions Associated with Increased Cardiovascular Hospitalizations. *Atmos. Environ.* **2013**, *74* (SupplementC), 320−325.
(34) Corbett, J. J.; Winebrake, J. J.; Green, E. H.; Kasibhatla, P.; Eyring, V.; Lauer, A. Mortality from Ship Emissions: A Global Assessment. *Environ. Sci. Technol.* **2007**, *41* (24), 8512−8518.
(35) Winebrake, J. J.; Corbett, J. J.; Green, E. H.; Lauer, A.; Eyring, V. Mitigating the Health Impacts of Pollution from Oceangoing Shipping: An Assessment of Low-Sulfur Fuel Mandates. *Environ. Sci. Technol.* **2009**, *43* (13), 4776−4782.
(36) Zhang, F.; Chen, Y.; Chen, Q.; Feng, Y.; Shang, Y.; Yang, X.; Gao, H.; Tian, C.; Li, J.; Zhang, G.; Matthias, V.; Xie, Z. Real-World Emission Factors of Gaseous and Particulate Pollutants from Marine Fishing Boats and Their Total Emissions in China. *Environ. Sci. Technol.* **2018**, *52* (8), 4910−4919.
(37) Fu, H.; Lin, J.; Shang, G.; Dong, W.; Grassian, V. H.; Carmichael, G. R.; Li, Y.; Chen, J. Solubility of Iron from Combustion Source Particles in Acidic Media Linked to Iron Speciation. *Environ. Sci. Technol.* **2012**, *46* (20), 11119−11127.
(38) Zhang, H.; Hu, D.; Chen, J.; Ye, X.; Wang, S. X.; Hao, J. M.; Wang, L.; Zhang, R.; An, Z. Particle Size Distribution and Polycyclic Aromatic Hydrocarbons Emissions from Agricultural Crop Residue Burning. *Environ. Sci. Technol.* **2011**, *45* (13), 5477−5482.
(39) Nisbet, I. C. T.; Lagoy, P. K. Toxic Equivalency Factors (Tefs) for Polycyclic Aromatic Hydrocarbons (Pahs). *Regul. Toxicol. Pharmacol.* **1992**, *16* (3), 290.
(40) Li, Q.; Jiang, J.; Qi, J.; Deng, J.; Yang, D.; Wu, J.; Duan, L.; Hao, J. Improving the Energy Efficiency of Stoves to Reduce Pollutant Emissions from Household Solid Fuel Combustion in China. *Environ. Sci. Technol. Lett.* **2016**, *3* (10), 369−374.
(41) Foldbjerg, R.; Dang, D. A.; Autrup, H. Cytotoxicity and Genotoxicity of Silver Nanoparticles in the Human Lung Cancer Cell Line, A549. *Arch. Toxicol.* **2011**, *85* (7), 743−50.
(42) Wu, D.; Zhang, F.; Lou, W.; Li, D.; Chen, J. Chemical Characterization and Toxicity Assessment of Fine Particulate Matters Emitted from the Combustion of Petrol and Diesel Fuels. *Sci. Total Environ.* **2017**, *605−606*, 172−179.
(43) Yue, H.; Yun, Y.; Gao, R.; Li, G.; Sang, N. Winter Polycyclic Aromatic Hydrocarbon-Bound Particulate Matter from Peri-Urban North China Promotes Lung Cancer Cell Metastasis. *Environ. Sci. Technol.* **2015**, *49* (24), 14484−93.
(44) Sun, J.; Shen, Z.; Zeng, Y.; Niu, X.; Wang, J.; Cao, J.; Gong, X.; Xu, H.; Wang, T.; Liu, H.; Yang, L. Characterization and Cytotoxicity of Pahs in Pm2.5 Emitted from Residential Solid Fuel Burning in the Guanzhong Plain, China. *Environ. Pollut.* **2018**, *241*, 359−368.
(45) Smith, A. M.; Durbic, T.; Oh, J.; Urbanus, M.; Proctor, M.; Heisler, L. E.; Giaever, G.; Nislow, C. Competitive Genomic Screens of Barcoded Yeast Libraries. *J. Visualized Exp.* **2011**, No. 54, 429−442.
(46) Escher, B. I.; Bramaz, N.; Mueller, J. F.; Quayle, P.; Rutishauser, S.; Vermeirssen, E. L. M. Toxic Equivalent Concentrations (Teqs) for Baseline Toxicity and Specific Modes of Action as a Tool to Improve Interpretation of Ecotoxicity Testing of Environmental Samples. *J. Environ. Monit.* **2008**, *10* (5), 612−621.
(47) Anderson, M.; Salo, K.; Hallquist, Å. M.; Fridell, E. Characterization of Particles from a Marine Engine Operating at Low Loads. *Atmos. Environ.* **2015**, *101*, 65−71.
(48) Kasper, A.; Aufdenblatten, S.; Forss, A.; Mohr, M.; Burtscher, H. Particulate Emissions from a Low-Speed Marine Diesel Engine. *Aerosol Sci. Technol.* **2007**, *41* (1), 24−32.
(49) Tao, Y.; Ye, X.; Jiang, S.; Yang, X.; Chen, J.; Xie, Y.; Wang, R. Effects of Amines on Particle Growth Observed in New Particle Formation Events. *J. Geophys. Res. Atmos.* **2016**, *121* (1), 324−335.
(50) Romagnoli, P.; Balducci, C.; Perilli, M.; Perreca, E.; Cecinato, A. Particulate Pahs and N-Alkanes in the Air over Southern and Eastern Mediterranean Sea. *Chemosphere* **2016**, *159*, 516−525.
(51) Simon, H.; Bhave, P. V.; Swall, J. L.; Frank, N. H.; Malm, W. C. Determining the Spatial and Seasonal Variability in Om/Oc Ratios across the Us Using Multiple Regression. *Atmos. Chem. Phys.* **2011**, *11* (6), 2933−2949.
(52) Turpin, B. J.; Lim, H.-J. Species Contributions to Pm2.5 Mass Concentrations: Revisiting Common Assumptions for Estimating Organic Mass. *Aerosol Sci. Technol.* **2001**, *35* (1), 602−610.
(53) Robert, M. A.; VanBergen, S.; Kleeman, M. J.; Jakober, C. A. Size and Composition Distributions of Particulate Matter Emissions: Part 1—Light-Duty Gasoline Vehicles. *J. Air Waste Manage. Assoc.* **2007**, *57* (12), 1414−1428.
(54) Li, X.; Xu, Z.; Guan, C.; Huang, Z. Particle Size Distributions and Oc, Ec Emissions from a Diesel Engine with the Application of in-Cylinder Emission Control Strategies. *Fuel* **2014**, *121*, 20−26.
(55) Watson, J. G.; Chow, J. C.; Lowenthal, D. H.; Pritchett, L. C.; Frazier, C. A.; Neuroth, G. R.; Robbins, R. Differences in the Carbon Composition of Source Profiles for Diesel- and Gasoline-Powered Vehicles. *Atmos. Environ.* **1994**, *28* (15), 2493−2505.
(56) Sippula, O.; Stengel, B.; Sklorz, M.; Streibel, T.; Rabe, R.; Orasche, J.; Lintelmann, J.; Michalke, B.; Abbaszade, G.; Radischat, C.; Groger, T.; Schnelle-Kreis, J.; Harndorf, H.; Zimmermann, R. Particle Emissions from a Marine Engine: Chemical Composition and Aromatic Emission Profiles under Various Operating Conditions. *Environ. Sci. Technol.* **2014**, *48* (19), 11721−11729.
(57) Shen, G.; Wang, W.; Yang, Y.; Ding, J.; Xue, M.; Min, Y.; Zhu, C.; Shen, H.; Li, W.; Wang, B.; Wang, R.; Wang, X.; Tao, S.; Russell,

DOI: 10.1021/acs.est.8b04471
Environ. Sci. Technol. 2018, 52, 12943−12951

A. G. Emissions of Pahs from Indoor Crop Residue Burning in a Typical Rural Stove: Emission Factors, Size Distributions, and Gas-Particle Partitioning. *Environ. Sci. Technol.* **2011**, *45* (4), 1206−1212.
(58) Cooper, D. A. Exhaust Emissions from Ships at Berth. *Atmos. Environ.* **2003**, *37* (27), 3817−3830.
(59) Zheng, X.; Zhang, S.; Wu, Y.; Xu, G.; Hu, J.; He, L.; Wu, X.; Hao, J. Measurement of Particulate Polycyclic Aromatic Hydrocarbon Emissions from Gasoline Light-Duty Passenger Vehicles. *J. Cleaner Prod.* **2018**, *185*, 797−804.
(60) de Abrantes, R.; de Assunção, J. V.; Pesquero, C. R. Emission of Polycyclic Aromatic Hydrocarbons from Light-Duty Diesel Vehicles Exhaust. *Atmos. Environ.* **2004**, *38* (11), 1631−1640.
(61) Lin, C.-C.; Chen, S.-J.; Huang, K.-L.; Lee, W.-J.; Lin, W.-Y.; Tsai, J.-H.; Chaung, H.-C. Pahs, Pah-Induced Carcinogenic Potency, and Particle-Extract-Induced Cytotoxicity of Traffic-Related Nano/Ultrafine Particles. *Environ. Sci. Technol.* **2008**, *42* (11), 4229−4235.
(62) Pham, C. T.; Kameda, T.; Toriba, A.; Hayakawa, K. Polycyclic Aromatic Hydrocarbons and Nitropolycyclic Aromatic Hydrocarbons in Particulates Emitted by Motorcycles. *Environ. Pollut.* **2013**, *183*, 175−183.
(63) Spezzano, P.; Picini, P.; Cataldi, D.; Messale, F.; Manni, C.; Santino, D. Particle-Phase Polycyclic Aromatic Hydrocarbon Emissions from Non-Catalysed, in-Use Four-Stroke Scooters. *Environ. Monit. Assess.* **2007**, *133* (1), 105−117.
(64) Contini, D.; Gambaro, A.; Belosi, F.; De Pieri, S.; Cairns, W. R. L.; Donateo, A.; Zanotto, E.; Citron, M. The Direct Influence of Ship Traffic on Atmospheric Pm2.5, Pm10 and Pah in Venice. *J. Environ. Manage.* **2011**, *92* (9), 2119−2129.
(65) Corbin, J. C.; Mensah, A. A.; Pieber, S. M.; Orasche, J.; Michalke, B.; Zanatta, M.; Czech, H.; Massabo, D.; Buatier de Mongeot, F.; Mennucci, C.; El Haddad, I.; Kumar, N. K.; Stengel, B.; Huang, Y.; Zimmermann, R.; Prevot, A. S. H.; Gysel, M. Trace Metals in Soot and Pm2.5 from Heavy-Fuel-Oil Combustion in a Marine Engine. *Environ. Sci. Technol.* **2018**, *52* (11), 6714−6722.
(66) Li, N.; Sioutas, C.; Cho, A.; Schmitz, D.; Misra, C.; Sempf, J.; Wang, M.; Oberley, T.; Froines, J.; Nel, A. Ultrafine Particulate Pollutants Induce Oxidative Stress and Mitochondrial Damage. *Environ. Health. Perspect.* **2002**, *111* (4), 455−460.
(67) Durga, M.; Nathiya, S.; Rajasekar, A.; Devasena, T. Effects of Ultrafine Petrol Exhaust Particles on Cytotoxicity, Oxidative Stress Generation, DNA Damage and Inflammation in Human A549 Lung Cells and Murine Raw 264.7 Macrophages. *Environ. Toxicol. Pharmacol.* **2014**, *38* (2), 518−530.
(68) Hemmingsen, J. G.; Møller, P.; Nøjgaard, J. K.; Roursgaard, M.; Loft, S. Oxidative Stress, Genotoxicity, and Vascular Cell Adhesion Molecule Expression in Cells Exposed to Particulate Matter from Combustion of Conventional Diesel and Methyl Ester Biodiesel Blends. *Environ. Sci. Technol.* **2011**, *45* (19), 8545−8551.
(69) Petzold, A.; Weingartner, E.; Hasselbach, J.; Lauer, P.; Kurok, C.; Fleischer, F. Physical Properties, Chemical Composition, and Cloud Forming Potential of Particulate Emissions from a Marine Diesel Engine at Various Load Conditions. *Environ. Sci. Technol.* **2010**, *44* (10), 3800−3805.

DOI: 10.1021/acs.est.8b04471
Environ. Sci. Technol. 2018, 52, 12943−12951